EJFA Emirates Journal of Food and Agriculture

Emirates Journal of Food and Agriculture 37: 1–12
doi: 10.3897/ejfa.2025.126332

RESEARCH PAPER

Mathematical models and ANFIS for determination of diffusivity and activation energy of button mushroom thin layer drying

Maryam Karimi Motlagh[1], Babak Beheshti[2], Ali Mohammad Borghei[2], Mohammad Gholami Parashkoohi[3]

1 *Department of Agricultural Mechanization Engineering, SR.C., Islamic Azad University, Tehran, Iran*
2 *Department of Biosystems Engineering, SR.C., Islamic Azad University, Tehran, Iran*
3 *Department of Mechanical Engineering, ShQ.C., Islamic Azad University, shahr-e Qods, Iran*

Corresponding author: Babak Beheshti (Beheshti-b@iau.ac.ir)

Academic editor: Mohamed Neji ♦ **Received** 27 April 2024 ♦ **Accepted** 18 April 2025 ♦ **Published** 31 July 2025

Abstract

In this research, four temperature levels of 50, 60, 70, and 80 °C with a constant airflow rate of 1 (m/s). To select an appropriate drying model, 16 thin-layer drying models and Neuro-Fuzzy Inference System (ANFIS) were used. To determine the best thin-layer mathematical model, nonlinear regression analysis was employed, utilizing indices such as R^2, χ^2, RMSE, and MRDM. The R software version 3.6.2 was used. The results indicated that among the mathematical models, the two-term model provided the best fit. The effective moisture diffusivity for the four temperatures ranged ($3.228942E^{-10}$ to $1.065814E^{-09}$) m^2/s. Significant changes of color were observed in ΔE concerning temperature. ΔE and Shrinkage increased with temperature, while SI and Hue angle values decreased with temperature.The activation energy value was 2277.341 (kJ/kg). according to the ANFIS results, the Two-term model was the most appropriate for drying the thin layer of button mushrooms, with the highest correlation coefficient (R^2 = 0.999) and root mean square error (RMSE = 0.001) compared to other models.

Keywords

ANFIS, Button Mushroom, Drying kinetics, Mathematical Model, Activation Energy

Introduction

Edible button mushroom (white button mushroom) *Agaricus bisporus*, is the second most cultivated mushroom globally (Kotwaliwale et al. 2007). This type of mushroom has the ability to grow in various temperature conditions and on different lignocellulosic materials (Talebian Masoudi et al. 2019). Edible mushrooms are produced and consumed in over a hundred countries worldwide. According to the statistics of the past decade, approximately 11 million tons of mushrooms were produced globally, with China leading by producing over 7,800,000 tons, ranking first in production followed by the United States with 420,000 tons, Italy with 683,000, the Netherlands with 300,000, Poland with 260,140, Spain with 197,000, and Iran with 180,000 tons. Iran wa ranked seventh in mushroom production, contributing approximately one percent of global production. The global cultivation area for this plant was 31,500 hectares (FAO 2021). Button mushrooms are valuable agricultural products, but their quality diminishes due to various factors from at the time of harvest. To prevent waste and increase their shelf life, various processing methods are used, with drying as one of the most important methods (AmirNejat 1994). Drying refers to the most prevalent process for preserving agricultural products (Mühlbauer 2020). In drying methods, factors like temperature, airflow rate, initial and final product

Copyright *Karimi Motlagh, et al.* This is an open access article distributed under the terms of the Creative Commons Attribution License (CC-BY 4.0), which permits unrestricted use, distribution, and reproduction in any medium, provided the original author and source are credited.

moisture, relative humidity, ambient air temperature, and food depth affect the rate of moisture change over time, or the drying kinetics, effectively (Wan Daud 2008). In mathematical models, variables and sets of dependent equations show the effect of independent variables in the real world, making this method highly suitable for predicting changes (Ziaforoughi et al. 2016). The Adaptive Neuro-Fuzzy Inference System (ANFIS) is one of the key artificial intelligence methods. In natural processes, ANFIS has operated successfully with evaluations and practical inquiries and has superiority over many statistical methods. Compared to linear regression models, ANFIS maintains the actual data prediction value (Tavakolipour et al. 2014). Furthermore, a study assessed the kinetics modeling of drying button mushrooms in a hot air convection dryer using a genetic algorithm-artificial neural network method. The effect of drying air temperature at three levels (50, 60, and 70 °C) and airflow velocity at three levels (1, 2, and 3 m/s) on button mushroom drying was examined. Based on the results, drying button mushrooms with hot air increased the drying rate with rising temperature and airflow velocity. Sensitivity analysis by the optimized network revealed that the dryer temperature was the most effective factor in controlling the sample weight reduction (Salehi et al. 2017). Therefore, this research is aimed at evaluating the parameters affecting the thin-layer drying process of button mushrooms, particularly temperature, and its impact on drying time and rate. Moreover, moisture variations during drying were analyzed by means of 16 different mathematical models and ANFIS prediction. Additionally, the quality attributes of button mushrooms such as their color quality and rumple were examined.

Materials and methods

The research was conducted on the Button mushroom, Moisture was measured before and after the Button mushroom was dried. The dryer used in the research was a 12-ft3 dryer manufactured by the Iran Grook Engineering Company. One meter per second of air velocity was maintained throughout the studies at 50, 60, 70, and 80 °C . A Japanese model digital scale (AND-EK-600, accuracy ±0.001 gr) was used to record the weight fluctuations of button mushroom samples that were removed from the dryer at 10-minute intervals. Drying was continued until the Button mushroom moisture reached 10% dryness. All experiments were performed in three replicants, and their averages were used in calculations and curve plotting (Salehi et al. 2017).

Equation (1) provided an expression for the samples' moisture ratio during drying:

$$\mathrm{MR} = \frac{\mathrm{M}_t - \mathrm{M}_e}{\mathrm{M}_0 - \mathrm{M}_e} \quad (1)$$

This equation may be used to calculate the moisture content at any stage throughout the drying process, as well as the equilibrium moisture content and the moisture content of samples in relation to their initial moisture content. However, as M_e's value is smaller than M or M_0's, the moisture ratio was simplified to M/M0 rather than $(M - M_e)/(M_0 - M_e)$ (Eshtiagh and Zare 2015). Parameters R^2, MRDM, RMSE and χ^2, nonlinear regression was used in R software (Statistical Package, version 3.6.3). (R^2) served as one of the main selection criteria for the optimal model. The quality of the fit was assessed using other statistical measures, including (χ^2), (MRDM), and (RMSE). Generally speaking, a greater R^2 value and lower χ^2, MRDM, and RMSE indicate a better fit (Guarte 1996).

The results were evaluated in order to identify a suitable model for explaining the drying process of button mushrooms (Table 1). The following equations are found in Table 2 and were utilized to calculate these parameters:

Table 1. Models used to investigate the Button mushroom thin layer drying.

No.	Model Name	Model
1	Newton	$MR = exp(-kt)$
2	Page	$MR = exp(-kt^n)$
3	Henderson and Pabis	$MR = a\ exp(-kt)$
4	Modified Henderson and Pabis-I	$MR = a\ exp(-k_0t) + b\ exp(-k_1t) + c\ exp(-k_2t)$
5	Modified Henderson and Pabis-II	$MR = a\ exp(-kt^n) + b\ exp(-gt) + c\ exp(-ht)$
6	Modified Page-I	$MR = a\ exp[-(kt^n)]$
7	Modified Page-II	$MR = exp[-(kt^n)]$
8	Modified Page-III	$MR = exp\text{-}(kt^n)$
9	Logarithmic	$MR = a\ exp(-kt) + c$
10	Two-term	$MR = a\ exp(-k_0t) + b\ exp(-k_1t)$
11	Mod. two-term-I	$MR = a\ exp(-k_0t) + (1 - a)\ exp(k_1t)$
12	Mod. two-term-II	$MR = a\ exp(-k_0t) + a\ exp(-k_1t)$
13	Mod. two-term-III	$MR = a\ exp(-k_0t^n) + b\ exp(-k_1t)$
14	Two-term exponential	$MR = a\ exp(-kt) + (1 - a)exp(-kat)$
15	Verma et al.	$MR = a\ exp(-kt) + (1 - a)exp(-gt)$
16	Diffusion approximation	$MR = a\ exp(-kt) + (1 - a)exp(-kbt)$

The Button mushroom moisture drying rate was calculated by Eq. (2) (Ozbek 2007).

$$\mathrm{DR} = \frac{M_t - M_{t+\Delta t}}{\Delta t} \quad (2)$$

Moisture diffusivity and activation energy

Using Fick's diffusion equation, the effective moisture diffusivity was determined. Equation (3):

$$\mathrm{MR}\frac{8}{\pi^2}\sum_{n=0}^{\infty}\frac{1}{(2n+1)^2}\exp\left(-\frac{(2n+1)^2\pi^2 D_{eff}^t}{l^2}\right) \quad (3)$$

The effective moisture diffusivity, Deff, was calculated by graphing Ln (MR) against the experimental drying time and analyzing the slope. The Arrhenius equation Eq. (4) may be used to connect Deff to temperature:

Table 2. Models evaluation indices.

Model name	Index
$X^2 = \frac{\sum_{i=1}^{N}(m_{Pi} - m_i)^2}{N - n}$	Chi-square
$\mathrm{RMSE} = \sqrt{\frac{\sum_{i=1}^{N}(m_i - m_{Pi})^2}{N}}$	(RMSE) Root Mean Square Error
$\mathrm{MRDM\%} = \frac{100}{N}\sum \frac{\lvert m_i - m_{Pi}\rvert}{m_i}$	Mean Relative Deviation Modulus (MRDM)
$R^2 = 1 - (\mathrm{Re\ sidual\ SS})/(\mathrm{Corrected\ total\ SS})$	Coefficient of Determination (R^2)

$$\mathrm{Ln}D_e = \ln D_0 - \left(\frac{E_a}{R}\right)\left(\frac{1}{T}\right) \quad (4)$$

Similar to this, data may be plotted in terms of Ln (Deff) vs. 1/T to obtain the activation energy from the slope of the line (Sun et al. 2007).

The relationship between diffusivity and temperature was calculated by Arrhenius equation from Equation (8) (Sun et al. 2007) and activation energy can be derived by Mujumdar (2000).

$$D_e = D_0 \exp\left(-\frac{E_a}{RT}\right) \quad (5)$$

$$\mathrm{Ln}D_e = \ln D_0 - \left(\frac{E_a}{R}\right)\left(\frac{1}{T}\right) \quad (6)$$

where D_0 is Arrhenius constant or the constant equivalent to the diffusivity at infinitely high temperature ($m^2\ s^{-1}$), R is the universal gas constant (8.314×10^{-3} kJ mol^{-1} k^{-1}), (T) is the absolute temperature (k), and E_a is the activation energy (kJ mol^{-1}).(Salehi 2016).

Artificial neural fuzzy inference system

Using a hybrid strategy based on both approaches or the least squares approach in conjunction with the backpropagation technique, it is feasible to ascertain the parameters of the first-order Takagi-Sugeno reasoning network. The ANFIS idea consists of five levels: Layer I is the fuzzy layer; Layer II is the rule layer; Layer III is the normalization layer; Layer IV is the defuzzification layer; and Layer V is the output layer. Each of the aforementioned levels processes the incoming signals in turn, with the last layer producing the final output. More specifically, the fuzzy if-then rules may be written as follows: Eq. (7) (Kashaninejad et al. 2007) using the ANFIS model with two inputs (x and y) and one output (f) as an example:

Rule $_1$: If x is A_1 and y is B_1; then $f_1 = p_1x + q_1y + r_1$ (7)

Rule $_2$: If x is A_2 and y is B_2; then $f_2 = p_2x + q_2y + r_2$ (8)

where the linguistic labels are A_1, A_2, B_1, and B_2, the first-order polynomials are f1 and f2, and the linear coefficients of the output function are p_1, p_2, q_1, q_2, r_1, and r_2. The input variables are transformed into a fuzzy set in Layer I (fuzzification) using membership functions. The corresponding node function for each of the adaptive nodes in Layer I is given by equations (9) and (10):

$$O^1_{Ai} = \mu_{Ai}(X)_i = 1, 2 \quad (10)$$

$$O^1_{Bj} = \mu_{Bj}(Y)_j = 1, 2 \quad (11)$$

The membership functions, denoted by lAi and lBj, are subject to shape variation. Subsequently, all incoming signals in Layer II (the rule layer) undergo multiplication by one another, with the outputs arriving in the general form Eq. (12):

$$\mathrm{O^2_i}\ \mathrm{w_i}\mu_{Ai}(X) * \mu_{Ai}(Y), \ldots_{i=1,2} \quad (12)$$

The entire firing strength is standardized in layer III (normalization) using Equation 13:

$$O^3_i = Wi = \frac{Wi}{W1 + W2} \quad (13)$$

where wi denotes the strength normalized. The defuzzification process is carried out by Layer IV to correlate the inputs and outputs. Equation (14):

$$O^4_i = \mathrm{W_i}f_i = \mathrm{W_i}\,(P_{iX} + \mathrm{qiY} + \mathrm{ri}) =_{i=1,2} \quad (14)$$

The coefficients of fi are represented by pi, qi, and ri. Finally, layer V, or output, compiles all of the incoming signals, and the total output is calculated using Eq. (15):

$$O^5_i = \sum \mathrm{i}\ \mathrm{W\,i}\ fi = \frac{\sum i\ \mathrm{W\,i}\ fi}{\sum i\ \mathrm{W\,i}}_{i=1,2} \quad (15)$$

In this research, the artificial neural network model of ANFIS using the Neural Network Toolbox in R ver.3.6.2 was also used to perform analysis for designing and predicting button mushroom moisture.

Color

The color of the Button mushroom sample was determined before and after drying at 50, 60, 70, and 80 °C using CLE L*a*b* color mode by colorimeter (3nh, model

NR10QC, Shenzhen, China), and the parameters L*, a*, b* were determined. Color indices were calculated by Eqs. (16)-(19) (Tahmasbpour et al. 2014).

$$\Delta l^* = l_2^* - l_1^* \tag{16}$$

$$\Delta a^* = a_2^* - a_1^* \tag{17}$$

$$\Delta b^* = b_2^* - b_1^* \tag{18}$$

$$\Delta E^* = \sqrt{(\Delta l^*)^2 + (\Delta a^*)^2 + (\Delta b^*)^2} \tag{19}$$

in which ΔE is the total amount of color change of the samples, and ΔL^*, Δa^*, and Δb^* are L*, a*, and b* changes due to temperature changes (Salehi et al. 2017).

The saturation index indicates the degree of color saturation and shows the color resistance to change, calculated by Eq. (20) (Akbarpour et al. 2016).

$$\mathrm{Sl} = \sqrt{(a^{*2} + b^{*2})} \tag{20}$$

The hue angle is used to describe food color. For example, red is represented by angles 0 or 360 degrees, and yellow, green, and blue are represented by angles 90, 180, and 270 degrees, respectively. It was calculated by Eq. (21) (Doymaz 2011).

$$\mathrm{HA} = \tan^{-1}\left(\frac{b^*}{a^*}\right) \tag{21}$$

Shrinkage

Shrinkage was calculated by Eq. (22) (Bingol et al. 2012).

$$\mathrm{S\%} = \left(\frac{\mathrm{V}}{\mathrm{V0}}\right) * 100 \tag{22}$$

Where S is the shrinkage, v is the Button mushroom volume at any time, and v_0 is the initial Button mushroom volume.

Results and discussion

Fig. 1, the slope of the drying curve has increased with increasing temperature, so that at 80 °C the curve has decreased with a steep slope. Approximately For every 10 degrees of temperature increase, the time to reach the final moisture content of 10% (db) reduced 100 minutes. By increasing the drying temperature, the evaporation potential increases and causes a rapid decrease in Button Mushrooms moisture content and drying time.With increasing the temperature from 50 to 60, 70, and 80 °C, the drying time decreased from About 610 to 480, 360, and 210 minutes, respectively. This response is attributed to the increase in the evaporation rate of button mushroom moisture. It also decreased with increasing drying time, which was more intense at higher temperatures. In terms of time efficiency, button mushroom drying was from 200 minutes to 600 minutes.

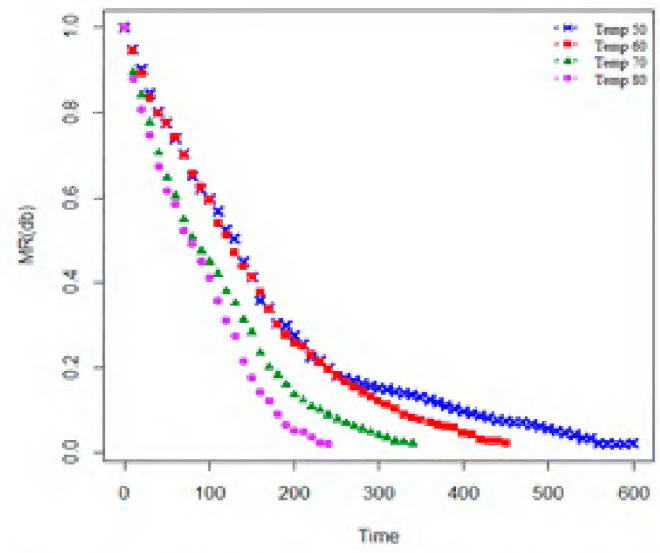

Figure 1. Button Mushrooms drying curves at various temperatures (50, 60, 70, and 80 °C).

Drying rate curves at temperatures from 50 to 80 °C

The Fig. 2, in Button Mushrooms drying at different temperatures has occurred at a falling rate period. Dried surface of the Button Mushrooms in the last sta ges of drying, creates a resistance in moisture transfer to the surface of the in Button Mushrooms, which reduces the drying rate in the final stages of drying (Kashaninejad et al. 2007). The linear regression equation of the drying rate was determined as a function of moisture content at different temperatures, which is given next to the diagram. These linear equations have a good fit with respect to the value of R^2. According to these equations, the slope coefficient of the regression line equation increases with increasing temperature and this the drying rate increases with increasing temperature.

The results of the drying rate equation at different temperatures

The equation of drying speed at different temperatures (50, 60, 70 and 80 °C) equal to (y=drying speed) and (X=humidity) is reported in Table 3. According to Table 3, it can be seen that button mushroom drying speed is slower at 50 temperature and humidity is high, and button mushroom drying speed is high at 80 temperature and humidity is low. Drying the mushroom shows the nutritional value of the mushroom. The process of drying mushrooms can significantly improve the nutritional properties of this product and improve its quality (Belyaeva et al. 2020).

Table 3. Regression equation of drying rate at different temperatures.

Temperature (°C)	Regression line equation	R^2
50	Y =0.0053x-0.3202	**0.9546**
60	Y =0.0089x-0.3815	**0.9786**
70	Y =0.0162x-0.4624	**0.9567**
80	Y = 0.0143x+0.1657	**0.9787**

Y = (Drying rate) X =(moisture content).

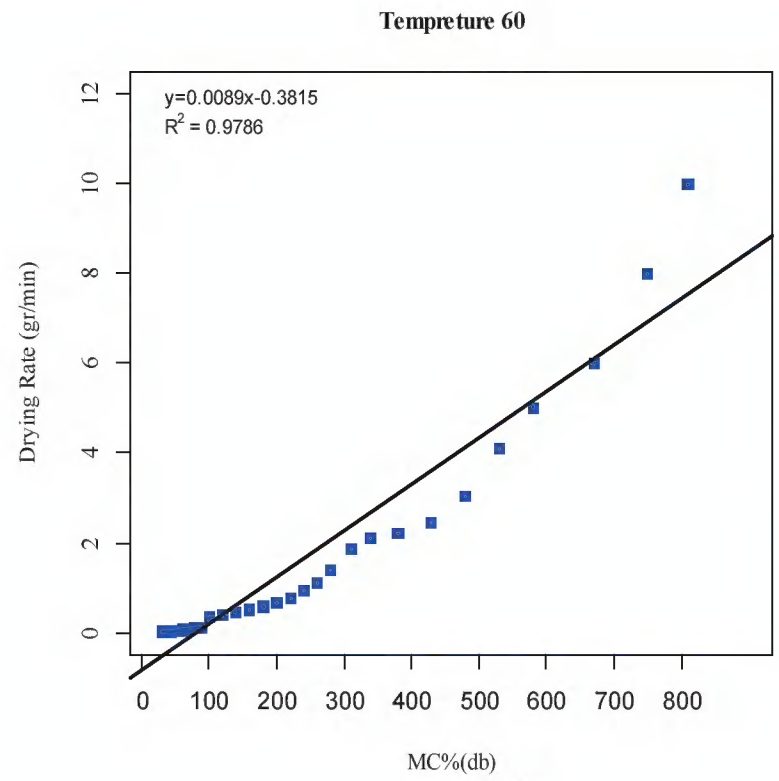

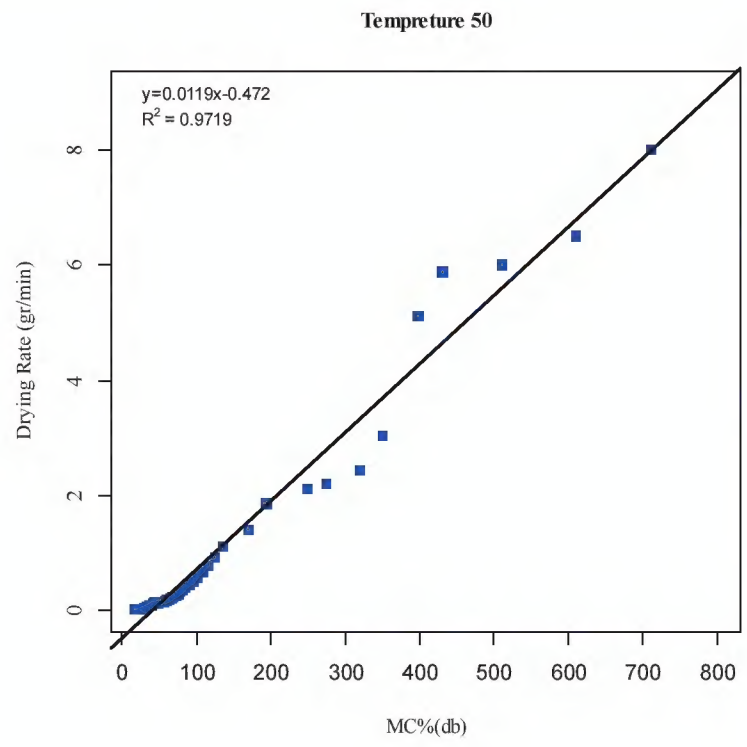

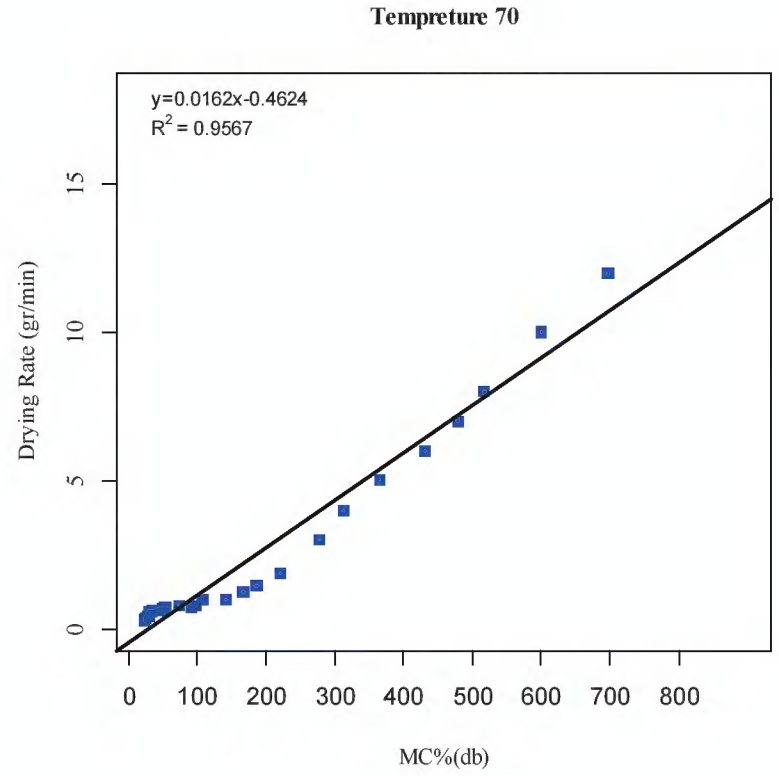

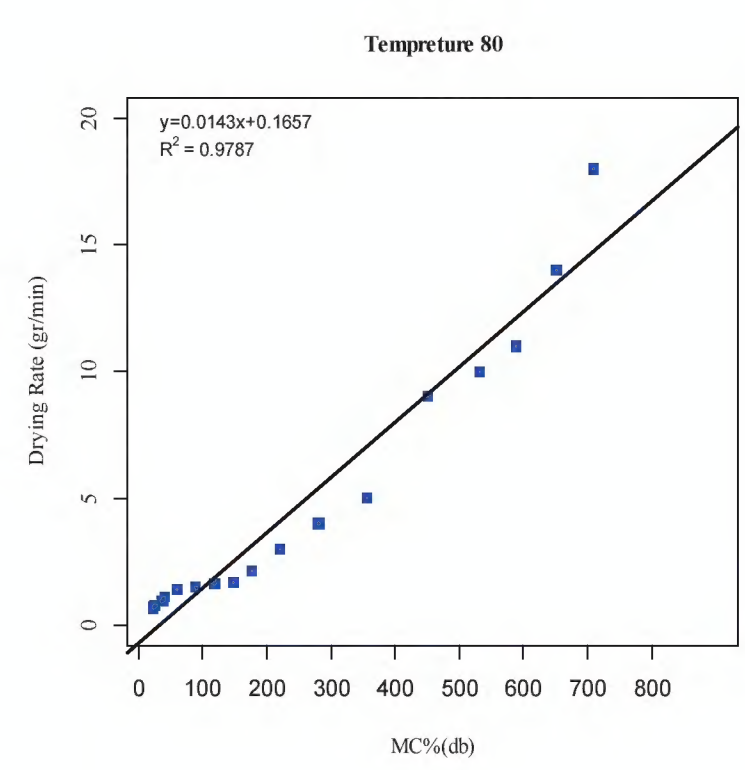

Figure 2. A drying rate curve at 50 °C, a drying rate curve at 60 °C, a drying rate curve at 70 °C, and a drying rate curve at 80 °C show the trend of variations in drying rates at various temperatures.

Selection of thin layer drying model

Based on Table 1, sixteen thin-layer models were fitted with data from dried button mushrooms. An analysis of the model assessment indices led to the selection of the two-term model as the optimal model. Table 4 lists this model's evaluation index values at various temperatures. Additionally, the two-term model's parameter values at various temperatures are shown in Table 5. (Kaur et al. 2008).

Table 4. Findings on the model constant parameters at various temperatures (50, 60, 70, and 80 °C) for the experiments.

Model Name		K1	K2	A	B
Two term	50	-6.652e-05	1.041e-04	2.918e-04	1.037e+00
	60	4.002e-04	1.094e-04	-1.432e-01	1.130e+00
	70	-3.000e-04	1.396e-04	-1.808e-05	9.931e-01
	80	-4.727e-04	1.443e-04	-2.345e-06	9.776e-01

Evaluation results of two-term model

The two-term model's assessment diagrams regarding the data collected are displayed in Fig. 3. The graphs show that the model fits the results of experiments rather well.

Table 5. Outcomes of fitting the two-term nonlinear model in the experimental approaches (0.05).

Model	T(°C)	MRDM%	x^2	RMSE	R^2
Two term	50	12.23954	0.0004749791	0.02106734	0.992
	60	5.439421	8.680308e-05	0.008983966	0.998
	70	4.678153	0.0001614895	0.01205573	0.997
	80	7.425246	0.0003759172	0.01824706	0.995

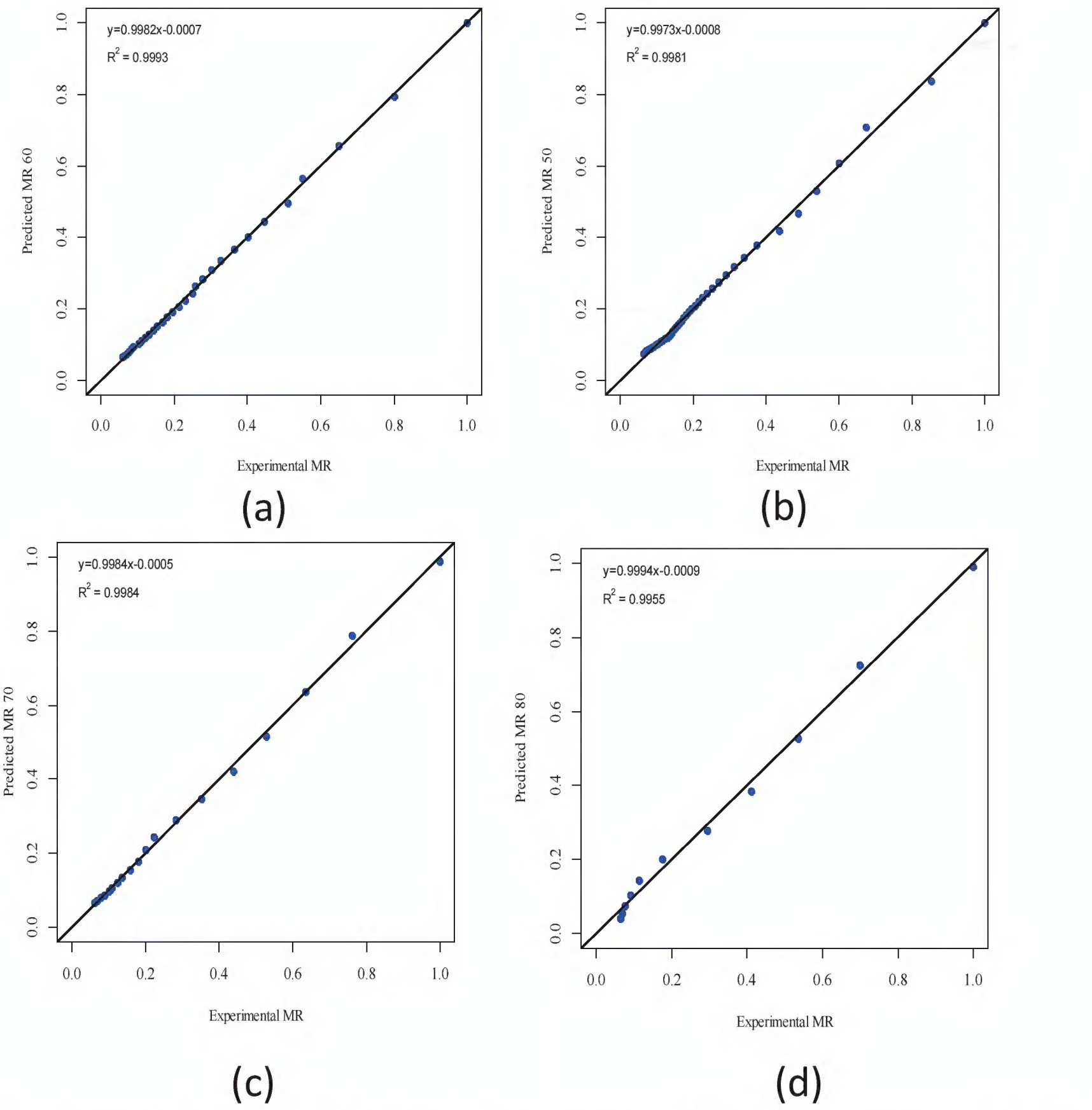

Figure 3. The comparison of the two-term model with experimental data at different temperatures (50, 60, 70, and 80 °C); (**a**) The comparison of the two-term model with experimental data at 50 °C, (**b**) The comparison of the two-term model with experimental data at 60 °C, (**c**) The comparison of the two-term model with experimental data at 70 °C, (**d**) The comparison of the two-term model with experimental data at 80 °C.

Results of effective moisture diffusivity at different temperatures

The effective diffusivity values at various experimental temperatures (50, 60, 70, and 80 °C) are displayed in Table 6. Since diffusivity was influenced by temperature, the effective moisture diffusivity rose as a result. The new study's findings align with those of previous investigations. Effective diffusivity values for food and agricultural products have been found by researchers to be between 10^{-9} and 10^{-11} m^2/s (Doymaz 2011). The Arrhenius equation illustrates in a different study how radiation levels and drying air temperature affect effective diffusivity in Eq. (10). These findings align with those of other investigators (Kaveh and Amiri Chayjan 2016).

Activation energy results

Changes in the moisture diffusivity can also have a direct effect on the amount of activation energy (Fig. 4). Table 7 shows the amount of activation energy and correlation coefficient. and its value was obtained from the angle coefficient of the regression line of 2277.3 (kJ/kg) (Kaveh and Amiri Chayjan 2016).

Table 6. Effective moisture diffusivity at different temperatures (50, 60, 70, 80 °C).

$D_{eff}*10^{-10}$ (m^2/S)	Temperature (c°)
0.01627763	50°
0.01731639	60°
0.02432949	70°
0.02834497	80°

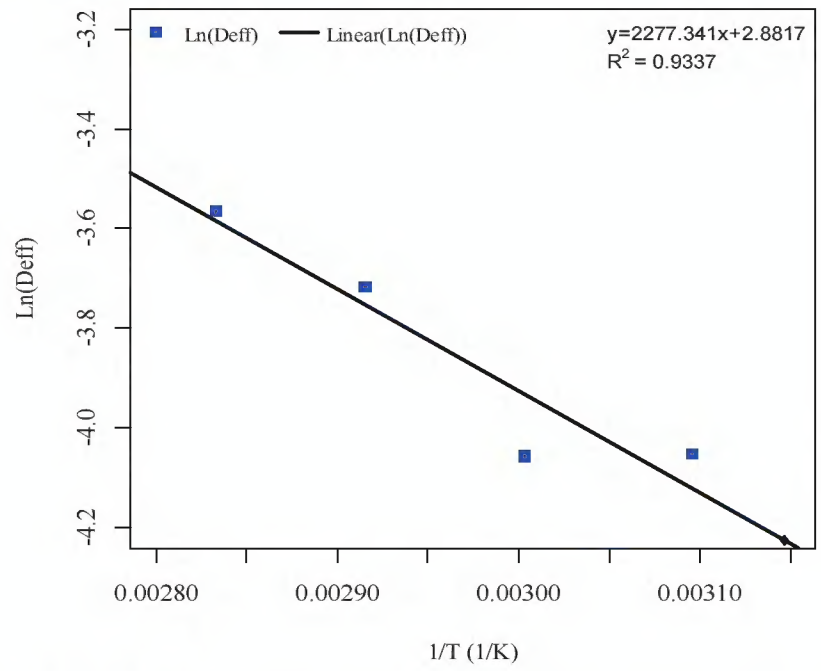

Figure 4. The amount of Button mushroom activation energy.

Changes in the moisture diffusivity Table 6 can also directly affect the amount of activation energy (Fig. 4) shows the amount of activation energy and correlation coefficient (Table 7) (Mohsenin 1986).

Table 7. The amount of Button Mushroom activation energy.

R^2	DO	*Ln_D0*	Activation energy (kJ/(kg.K) E	Eq.
0.9337	17.845	2.8817	2277.341	Y = 2277.341X-2.8817

Quality results of button mushroom (shrinkage and color)

Using the aov function in the stat package, a one-way analysis of variance was carried out to fit the findings of each qualitative dependent variable in three repeats at the 5% level. Using the aov function in the stat package, a one-way analysis of variance was carried out to fit the findings of each qualitative dependent variable in three repeats at the 5% level. And also to perform pairwise comparisons and identify homogeneous groups, the agricolae package was used, and also to draw different graphs, the ggplot 2 package was used.

Results on shrinkage

The shrinkage results showed that the effect of temperature was significant on shrinkage. The button mushroom shrinkage increased with increasing drying temperature and as a result of decreasing moisture content. It can be stated that with moisture release, viscoelastic stresses in the pores decrease, and as a result, button mushroom shrinkage increases (Vazquze et al. 1997). As the drying temperature rose, button mushroom shrinkage reduced. As the drying heat of the mushrooms rose, it was observed that the shrinkage of button mushrooms decreased (Fig. 5). The dryer's shrinkage increased when the temperature dropped from 80 to 50 °C. Regarding the impact of process temperature on the shrinkage of dried samples, Hashim et al. (2014) have obtained comparable findings. The comparison results of the average shrinkage of button mushroom at different temperatures (50, 60, 70, 80 °C) were reported in Table 8 and Fig. 6.

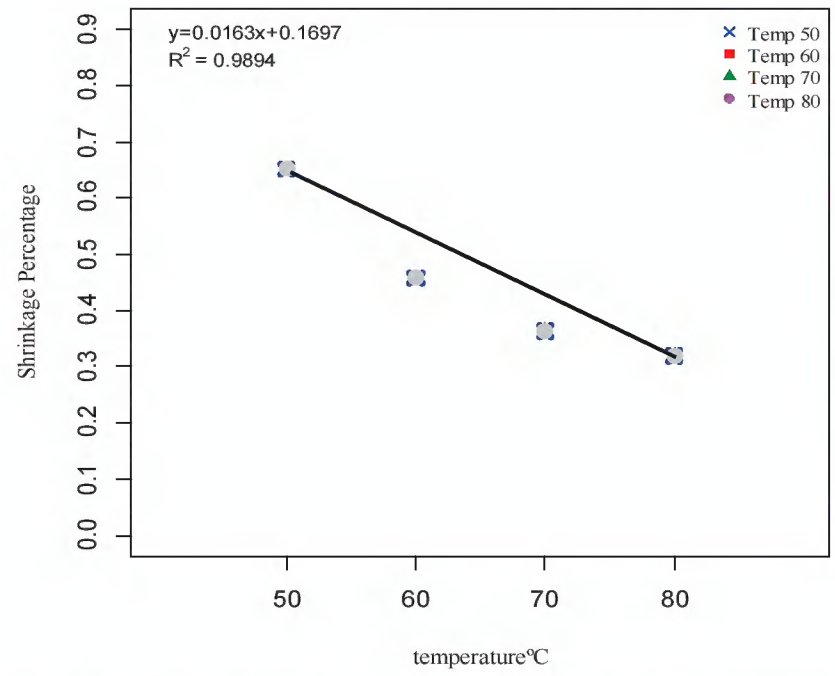

Figure 5. Shrinking of button mushroom at different temperatures (50, 60, 70, 80 °C).

Results on color

Color is considered one of the most important indicators in evaluating the quality of agricultural products, including food. The current research investigated the effects of drying temperatures on Quantitative or qualitative parameters, such as total color, changes ΔE, chroma index or saturation index (SI), and Hue angle index. Tables 9, 10 presents the results for the qualitative parameters of Button mushroom at different temperatures.

L* Index: the drying temperature significantly affects the color of button mushrooms, while the effect of air speed on the color changes of this product is not significant (Chung 2014). The change in color is due to the decrease in the lightness of the original samples and its effect on the L* factor or the brightness level. This indicates that with the increase in temperature, the button mushroom of the original samples tends to turn brown (Nour et al. 2011).

Table 8. The comparison results of the average shrinkage of button mushroom at different temperatures (50, 60, 70, 80 °C).

Color features	Sources of changes	Degrees of freedom	Error Degrees of freedom	Sum of squares Treatments	Error sum of squares	The total average of the treatments	Error Sum of averag	Sq F value	Pr (>F)
Button mushroom shriveling	Temperature	3	396	0.3271	0.9814	0.0015	0.5836	222	<2e-16

Statistics R 3.6.3.

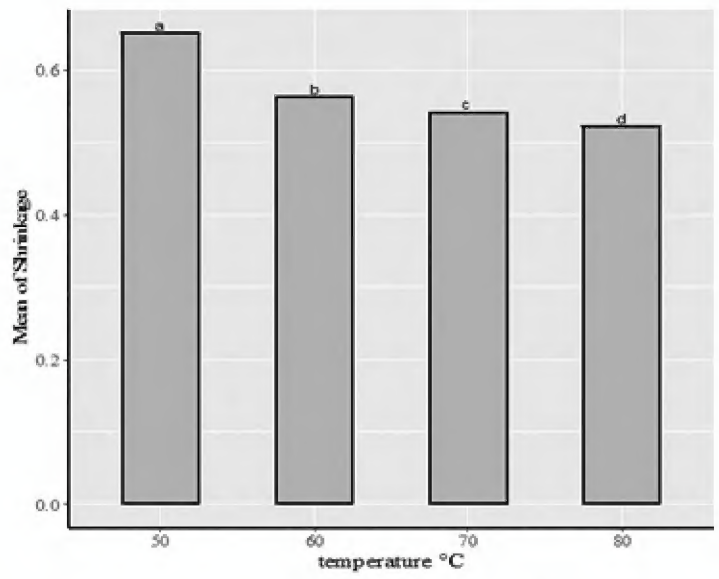

Figure 6. The results of the comparison of means for dried button mushrooms shrinkage at different temperatures (50, 60, 70, and 80 °C).

a* Index: is the result of variance analysis of redness-yellowness, which, if positive, indicates more redness in the sample. The value of parameter at different temperatures (50, 60, 70, and 80 °C) was reported as insignificant in the Table 10 (Gorjian 2011).

b* Index: the results of the analysis of variance of the yellowness index positivity indicate the yellowness of the sample. The value of parameter b* at different temperatures the value of parameter b* of the samples and the independent effect of different temperature conditions on button mushroom drying. It decreased significantly with the increase of temperature and process (Table 10).

ΔE index: The effect of different temperatures on button mushroom and also the interaction effect of these two factors on the value of ΔE in Table 9. In the roasted samples, changes in ΔE value increased with increasing temperature and its value decreased. Chung et al. reported that ΔE value increased with increasing temperature and its value increased in Figs 7–9 (Chung 2014).

SI index: the degree of saturation or color intensity of fresh button mushroom and button mushroom samples at temperatures decrease with increasing temperature of

Table 9. The results of b, a, L and test samples at different temperatures.

Type of treatment	L^*	a^*	b^*	SI	HA	ΔE
Fresh button mushrooms	78.39	4.74	15.85	16.54	73.36	78.39
50	56.23	11.05	23.04	25.57	64.4	56.23
70	52.56	8.21	19.48	21.14	67.13	52.56
60	49.41	13.97	31.69	34.63	66.21	49.41
80	48	16.8	32.74	36.79	62.84	48

Statistics R 3.6.3.

this index. The color resistance of the button mushroom is against the changes, which shows that the button mushroom shows less resistance to color change at high temperatures. The investigation of the independent effect of the parameters showed that the effect of low temperatures and the interaction effect of temperature on the intensity of color is not significant, but the effect of high temperature of polishing on the intensity of color in Tables 9, 10 similar results by Chung et al. showed that the color intensity increased with increasing drying temperature (Chung 2014).

HA index: The hue angle expresses the dominant color and the closer this angle is to zero, the whiter the sample is found and according to the Table 10 expressing the whiteness of the color of the button mushroom, which was reported to be significant.(Chand Mittal et al. 2012). The lowest amount of white color related to the dry sample at a temperature of 80 °C Table 8. With the increase in temperature from 50 to 80 °C, the Hue angle decreased by 2 degrees (Table 11). Garjian et al. Results a similar study reported that the color angle (H) increased with increasing temperature in the drying of thin layers (Gorjian 2011).

Results of fuzzy neural inference system (ANFIS)

The results of an experimental and applied study on ANFIS were used to predict the humidity ratio of the Button

Table 10. Results of variance analysis of quality parameters of dried button mushrooms at different temperatures.

Color features	Sources of changes	Degrees of freedom	Error Degrees of freedom	Sum of squares Treatments	Error sum of squares	The total average of the treatments	Error Sum of averages	F	P
L^*	Temperatures	4	10	1845	26.8	2.461	826.0	2e-16	886828
a^*	Temperatures	4	10	56.240	9.23	14.60	39.2	2e-16 9	53696
b^*	Temperatures	4	10	8.758	7.3	14914	71.189	2e-16	14914
ΔE	Temperatures	4	10	9.475	0.11	0.119	1.1	2e-16	4.3e-08
HA	Temperatures	4	10	04.113	8.31	261.28	8150	02/2e-13	1235
SI	Temperatures	4	10	1.873	1.873	3.218	3.218	2e-16	91715

Figure 7. Color change the fresh Button mushroom and the dried at different temperatures (50, 60, 70, and 80 °C).

Figure 8. Results on color quantitative parameters of investigation of Fresh button mushrooms and dried button mushroomsat different temperatures (50, 60, 70, 80 °C).

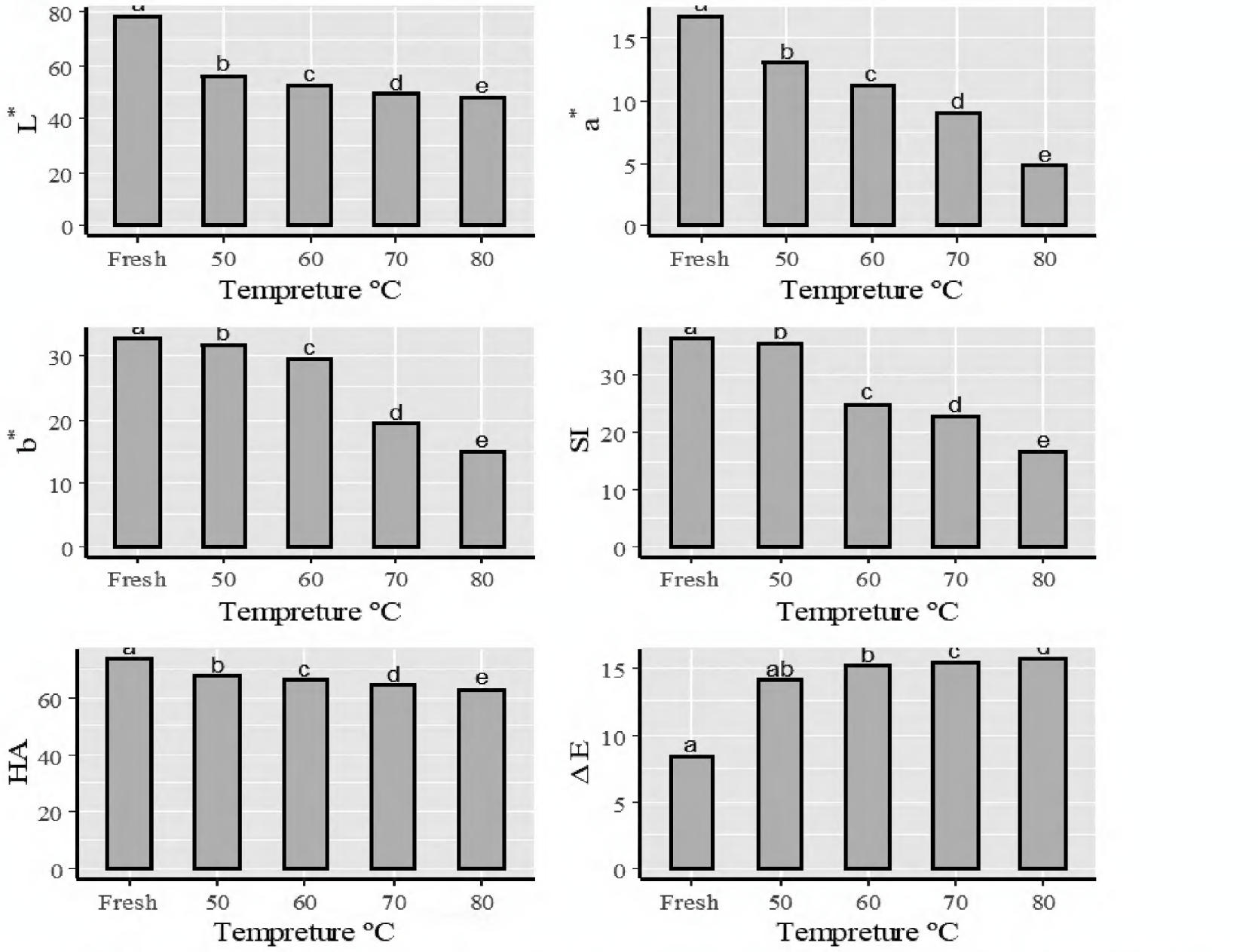

Figure 9. The results of the comparison of means for button mushrooms color variations at different temperatures (50, 60, 70, 80 °C).

Table 11. The impact of temperature in degrees on the qualitative traits of button mushrooms.

Qualitative parameters	Temperature			
Color parameters	50	60	70	80
L*	22.23	22.22	.20	54.19
a*	07.24	31.20	15.20	59.10
b*	90.8	53.7	15.6	51.4
SI	8269321.	08963.21	21.48096	1935.219
Hue	9977723.	5727623.	7424323.	21.079889
ΔE	84453.10	10.62145	15114110.	8.15178

mushroom. In this study, the results of data related to the best algorithms and results for predefinite are reported. ANFIS was used in analysis, like other models (Fig. 10). Different models of ANFIS have been designed using trial and error method. The results of ANFIS are summarized in Table 12, which shows that the minimum RMSE and the highest value of R^2 were provided by the ANFIS algorithm (Tavakolipour et al. 2014) drying time for Button Mushroom (240 min) occurred and the longest drying time occurred (600 min). The results of an experimental and applied study of ANFIS were used to predict the humidity ratio of But-

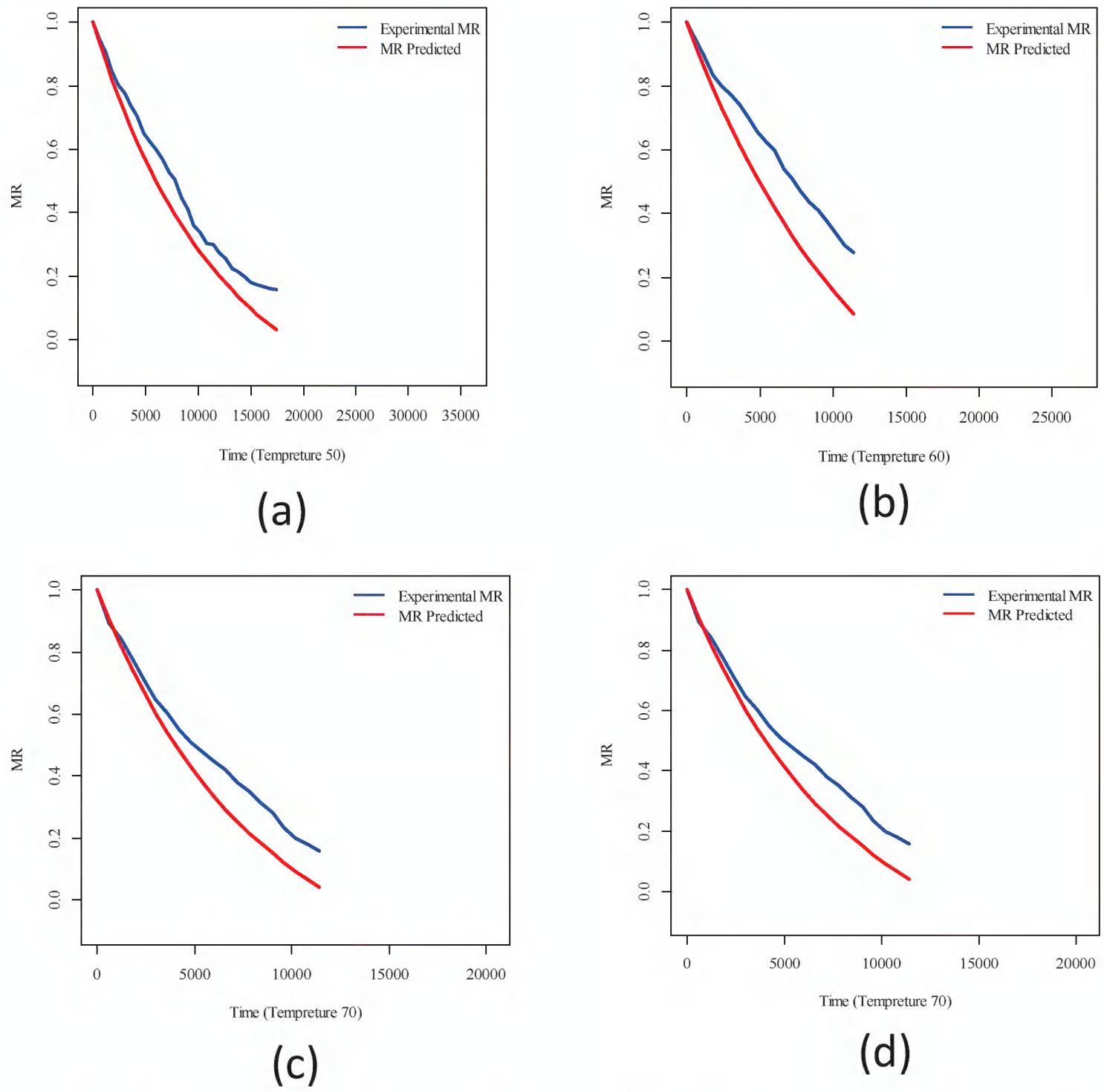

Figure 10. Determination of ANFIS to predict the moisture ratio of Button mushroom in four levels of temperature changes (50, 60, 70, 80 °C); (**a**) The determination of ANFIS to predict the moisture ratio of Button mushroom at temperature (50 °C), (**b**) The determination of ANFIS to predict the moisture ratio of Button mushroom at temperature (60 °C), (**c**) The determination of ANFIS to predict the moisture ratio of of Button mushroom at temperature (70 °C), (**d**) The determination of ANFIS to predict the moisture ratio of Button mushroom at temperature (80 °C).

ton mushroom. In this study, the results of data related to the best algorithms and results for predefinite are reported. In the analysis ANFIS, like other models used, was used. Different models of ANFIS have been designed using trial and error method. The results of ANFIS are summarized in Table 12. This table shows that the minimum RMSE and the highest value of R^2 are provided by ANFIS algorithm.

Table 12. ANFIS results for trimf membership function.

Function type	Number of functions	RMSE	R^2
Trimf	2-2-2	0.001	0.999
Gaussmf	2-2-2	0.002	0.999

Comparison of mathematical models and ANFIS

In this research, mathematical models and ANFIS were investigated to predict the moisture ratio of button mushroom. To determine the appropriate model, the highest R^2 value and the lowest RMSE were obtained. By comparing Tables 5, 9, the Anfis model in this research predicted the experimental data better than the mathematical models. They had similar results in the comparison of mathematical models and Anfis (Kaveh et al. 2019).

Conclusions

In this study, drying kinetics of button mushroom were investigated in dryer at different temperature levels. The obtained results are summarized as follows: As the temperature level increased, drying rate increased and drying time decreased. The two term model gave the best representations of drying data under all experimental conditions. The effective moisture diffusivity (De) for temperatures (50, 60, 70, and 80 °C) were obtained ($3.228942E^{-10}$, $3.969273E^{-10}$, $6.375493E^{-10}$ and $1.065814E^{-09}$) m^2/s, respectively. Activation energy was estimated by a modified Arrhenius-type equation and found to be 2277.3 kW/kg. As the temperature increased, shrinkage, SI, and HA color indices decreased, and the ΔE color index increased. The performance prediction result of the ANFIS the two term

model was higher than the Math models. Azimi-Nejadian and Moradi Hassan Abad 2020, reported a similar results. Therefore, the binomial model in the Fuzzy Neural Inference System (ANFIS) method showed the most appropriate prediction of button mushroom moisture ratio.

Nomenclature

MR	Humidity ratio (no dimension)
M_t	The amount of moisture in the product at any time
M_e	Equilibrium moisture content, % (b.d)
M_0	The amount of initial moisture, % (b.d)
DR	Drying rate
$M_t - M_{t+\Delta t}$	The amount of moisture in time ,% (b.d)
T	Drying time Min
$\chi 2$	Square kai
RMSE	The root of the mean square error
MRDM%	Average modulus of relative deviation
R^2	Explanation coefficient
k_1	Drying constant
k_2	Drying constant
a	Drying constant
b	Drying constant
C	Concentration (Mole / m^3)
θ	Time (s)
De	Effective penetration coefficient (m^2 / s)
Z	Spatial coordinate (m)
R	equivalent radius (m)
t	Drying time
E_a	Activation energy (KJ / mol)
D_0	Base penetration coefficient (m^2 / s)
R	constant gases (J / mol.k)
T(K)	Absolute temperature (K)
L	Length
W	Width
T	Thickness
V	Volume
a	Half diameter large
b	Medium
c	Small
S	Shrinkage
V	the final Volume
V_0	Initial volume
L*	Brightness
a*	Color purity
b*	Color purity
$E\Delta$	The total amount of color changes in the samples
SI	Color degree saturation index
HA	Hugh angle

Author contributions

Maryam Karimi Motlagh: Data curation, Methodology, Writing – original draft, Writing – review & editing. Babak Beheshti: Conceptualization, Formal analysis, Supervision, Validation. Alimohammad Borghaee: Resources, Software, Mohammad Gholami Parashkoohi: Investigation, Writing – review & editing.

References

Abasi S, Minaei S, Khoshtaghaza MH (2014) Investigation of kinetics and energy consumption of thin layer drying of corn. Journal of Agricultural Machinery 4(1): 97–107.

Akbarpour H, Mohajeri M, Akbarpour M (2016) Pore diameter of nanoporous anodic alumina: experimental study and application of ANFIS and MLR. Chemometrics and Intelligent Laboratory 153: 82–91. https://doi.org/10.1016/j.chemolab.2016.02.012

AmirNejat H, Khoshtaghaza MH, Pahlavanzadeh H (2011) A determination of thin layer drying kinetics of button mushroom when dried through an infrared applied drying method. Iranian Journal of Biosystem Engineering 42(1): 53–56.

Azimi-Nejadian A, Moradi Hassan Abad M (2020) Comparison of mathematical models, artificial neural networks and adaptive neuro-fuzzy inference system (ANFIS) in prediction of instantaneous drying curves of potato slices in a microwave dryer H. Food Engineering Research 19(68): 137–154.

Bingol G, Roberts JS, Balaban MO, Devres YO (2012) Effect of Dipping temperature and dipping time on drying rate and color change of grapes. Drying Technology: An International Journal 30(6): 597–606. https://doi.org/10.1080/07373937.2011.654020

Chung HS, Kim JK, Moon KD, Youn KS (2014) Changes in color parameters of corn kernels during roasting. Food Science and Biotechnology 23(6): 1829–1835. https://doi.org/10.1007/s10068-014-0250-x

Doymaz I (2011) Drying of eggplant slice in thin layers at different air temperatures. Journal of Food Processing and Preservation 35: 280–289. https://doi.org/10.1111/j.1745-4549.2009.00454.x

Eshtiagh A, Zare D (2015) Modeling of thin layer hot air-infrared drying of green peas. Agricultural Engineering International: CIGR Journal 23(4): 246–258.

FAO (2021) The State Of Food And Agriculture. [Retrieved from] http://faostat.fao.org/site/567/Desktop%20Default.aspx?PageID=567

Gorjian S, Tavakoli Hashtjin T, Khosh Taghaza MH, Nikbakht AM (2011) Drying kinetics and quality of Barberry in a thin layer dryer. Journal of Agricultural Sciencend Technology 13: 303–314.

Guarte RC (1996) Modeling the drying behavior of copra and development of a natural convection dryer for production of high quality copra in the Philippines. Ph.D. Thesis, Hohenheim, Stuttgart, Germany.

Hashim N, Daniel O, Rahaman E (2014) A preliminary study: Kinetic model of drying process of pumpkins (*Cucurbita moschata*) in a convective hot air dryer. Agriculture and Agricultural Science Procedia 2: 345–352. https://doi.org/10.1016/j.aaspro.2014.11.048

Hatamipour MS (2002) Shrinkage of carrots during drying in an inert medium fluidized bed. Journal of Food Engineering 55(3): 247–252. https://doi.org/10.1016/S0260-8774(02)00082-1

Kashaninejad M, Mortazavi A, Safekordi A, Tabil LG (2007) Thin-layer drying characteristics and modeling of pistachio nuts. Journal of

Food Engineering 78(1): 98–108. https://doi.org/10.1016/j.jfoodeng.2005.09.007

Kaur A, Kaur D, Oberoi DPS, Gill BS, Sogi DS (2008) Effect of dehydration on physicochemical properties of mustard, mint and spinach. Journal of Food Processing and Preservation 32: 103–116. https://doi.org/10.1111/j.1745-4549.2007.00168.x

Kaveh M, Amiri Chayjan R (2016) Modeling thin-layer drying of turnip slice under semi-industrial continuous band dryer. Journal of Food Processing and Preservation 41(2): e12778. https://doi.org/10.1111/jfpp.12778

Kaveh M, Jahanbakhshi A, Golpour I, Mesri Gandshmin T, Abbaspour-Gilandeh Y, Jahedi Rad Sh (2019) Prediction of white mulberry drying kinetics in microwaveconvective dryer: A comparative study between mathematical model, artificial neural network and ANFIS. Journal of Food Science and Technology 88(16): 201–219.

Kotwaliwale N, Bakane P, Verma A (2007) Changes in textural and optical properties of oyster mushroom during hot air drying. Journal of Food Engineering 78(4): 1207–1211. https://doi.org/10.1016/j.jfoodeng.2005.12.033

Mohsenin N (1986) Physical properties of plant and animal materials. Gordon and Breach Science Publishers.

Mühlbauer W (2020) Drying Atlas: Drying Kinetics and Quality of Agricultural Products. Woodhead Publishing, England. https://doi.org/10.1016/B978-0-12-818162-1.00002-X

Ozbek BA (2007) Thin-layer drying characteristics and modeling of mint leaves undergoing microwave treatment. Food Engineering 83: 541–549. https://doi.org/10.1016/j.jfoodeng.2007.04.004

Salehi F, Kashaninejad M, Najafi A, Asadi F (2017) Modeling the kinetics of thin-layer drying of button mushroom by hot air using genetic algorithm - artificial neural network. Journal of Food Research (Agricultural Science) 26(3): 457–467.

Sui Y, Yang J, Ye Q, Li H, Wang H (2014) Infrared, convective, and sequential in frared and convective drying of wine grape pomace. Drying Technol: An International Journal 32(6): 686–694. https://doi.org/10.1080/07373937.2013.853670

Sun J, Hu X, Zhao G, Wu J, Wang Z, Chen F, Liao X (2007) Characteristics of thin-layer infrared drying of apple pomace with and without hot air-drying. Food Science and Technology International 13: 91–97. https://doi.org/10.1177/1082013207078525

Tahmasbpour M, Dehghannia J, Seidlo Haris SS, Ghanbarzade B (2014) Modeling color changes during drying grapes are pretreated with ultrasound and carboxy methyl cellulose and its organoleptic characteristics. Journal of Food Technologies 1: 61–79. http://dx.doi.org/10.22104/jift.2014.44

Talebian Masoudi A (2019) A review of the results of research on the use of *Agaricus bisporus* mushroom spent compost in animals feeding. Applied Animal Science Research Journal 8(31): 11–20. https://doi.org/10.22092/aasrj.2019.123383.1163

Tavakolipour H, Mokhtarian M, Kalbasi-Ashtari A (2014) Intelligent monitoring of zucchini drying process based on fuzzy expert engine and ANN. Journal of Food Process Engineering 37(5): 474–481. https://doi.org/10.1111/jfpe.12101

Varasteh F, Arzani K, Barzegar M, Zamani Z (2012) Changes in anthocyanins in arils of chitosan-coated pomegranate (*Punica granatum* L. cv. Rabbab-e-Neyriz) fruit during cold storage. Food Chemistry 130: 267–272. https://doi.org/10.1016/j.foodchem.2011.07.031

Vazquze G, Chenlo F, Moreira R, Cruz E (1997) Grape drying in a pilot plant with a pump. Drying Technology 15(3): 899–920. https://doi.org/10.1080/07373939708917267

Wan Daud WR (2008) Fluidized Bed Dryers — Recent Advances. Journal Advanced-Powder-Technology 19(5): 4. https://doi.org/10.1163/156855208X336675

Ziaforoughi A, Yousefi AR, Razavi SMA (2016) A comparative modeling study of quince infrared drying and evaluation of quality parameters. International Journal of Food Engineering 12(9): 901–910. https://doi.org/10.1515/ijfe-2016-0074